

# Relativistic Calculation Of Two-Electron One-Photon And Hypersatellite Transition Energies For $12 \leq Z \leq 30$ Elements

M. C. Martins,<sup>1,2,\*</sup> A. M. Costa,<sup>1,2</sup> J. P. Santos,<sup>1,3</sup> F. Parente,<sup>1,2</sup> and P. Indelicato<sup>4</sup>

<sup>1</sup>*Centro de Física Atómica da Universidade de Lisboa,  
Av. Prof. Gama Pinto 2, 1649-003 Lisboa, Portugal*

<sup>2</sup>*Departamento Física, Faculdade de Ciências,  
Universidade de Lisboa, Campo Grande, 1749-016 Lisboa, Portugal*

<sup>3</sup>*Departamento de Física, Faculdade de Ciências e Tecnologia,  
Universidade Nova de Lisboa, Monte de Caparica, 2825-114 Caparica, Portugal*

<sup>4</sup>*Laboratoire Kastler-Brossel, École Normale Supérieure  
et Université Pierre et Marie Curie, Case 74,  
4 place Jussieu, F-75252 Paris CEDEX 05, France*

(Dated: March 5, 2018)

## Abstract

Energies of two-electron one-photon transitions from initial double K-hole states were computed using the Dirac-Fock model. The transition energies of competing processes, the  $K\alpha$  hypersatellites, were also computed. The results are compared to experiment and to other theoretical calculations.

PACS numbers: 31.25.Jf, 32.30Rj, 32.70.Cs

Keywords: Atomic Transition Energies, Two-electron One-photon Transitions, X rays, Hypersatellites and Satellites

---

\*Electronic address: mdmartins@fc.ul.pt

## I. INTRODUCTION

Energies and transition rates for some radiative processes in atoms initially bearing two K-shell holes (two-electron one-photon and one-electron one-photon transitions) were evaluated in this work. This kind of atom, in which an entire inner shell is empty while the outer shells are occupied, was first named hollow by Briand *et al.* [1]. Hollow atoms are of great importance for studies of ultrafast dynamics in atoms far from equilibrium and have possible wide-ranging applications in physics, chemistry, biology, and materials science [2].

A mono-ionized atom with a K-shell vacancy can decay through an  $L \rightarrow K$  electron transition with the emission of x-ray radiation called, in the Siegbahn notation, the  $K\alpha$  diagram line. A one-electron transition line for which the initial state has two vacancies in the same shell is called a hypersatellite line. This is the case when a double ionized K-shell state decays through the transition of one L-shell electron (Fig. 1-a),  $K^{-2} \rightarrow K^{-1}L^{-1}$ , which is denoted by  $K\alpha^h$ . A competing, less probable, process of radiative de-excitation from this state is the simultaneous transition of two correlated electrons from higher shells, the  $K^{-2} \rightarrow L^{-2}$  transitions, accompanied by the emission of a single photon carrying the total energy, called  $K\alpha\alpha$  (Fig. 1-b). Predictions of this decaying process can be found in early papers at the beginning of the twentieth century by Heisenberg [3] and Condon [4], but it has only been observed since 1975 [5, 6].

For comparison with theory, we should distinguish between experiments in which the initial atomic excitation uses electrons as projectiles [7, 8, 9], photoionization or nuclear decay [10], and experiments using heavy ions [5, 6, 11]. In the latter case, the probability of multiple ionization is usually very high, leading to unreliable determination of energy values. One of the reasons for the scarcity of accurate experimental data stems from the very low intrinsic probability of creating a state with just two K-shell holes.

Theoretical calculations so far have mainly used perturbation theory and were performed in a non-relativistic approach [12, 13] with the exception of Chen et al. work [14], in which a Dirac-Hartree-Slater approach was used. Indeed, for medium- $Z$  atoms the K-shell electrons are already significantly relativistic, thus calling for relativistic methods in atomic data calculations. In this work we used the Dirac-Fock model to compute transition energies for two-electron one-photon transitions arising from the de-excitation of double 1s hole states leading to final states with two L-shell holes in atoms with  $12 \leq Z \leq 30$ . This is the region

of atomic numbers where the transition from the LS to the intermediate coupling scheme occurs. This transition is reflected directly in the  $K\alpha^h$  lines relative intensities. We also computed the energies of the competing hypersatellite transitions. The results are compared to experiment and other theoretical calculations.

## II. CALCULATION OF ATOMIC WAVE FUNCTIONS AND ENERGIES

Bound state wave functions and radiative transition probabilities were calculated using the multi-configuration Dirac-Fock program of J. P. Desclaux and P. Indelicato [15, 16]. The program was used in single-configuration mode because correlation was found to be unimportant. The wave functions of the initial and final states were computed independently, that is, atomic orbitals were fully relaxed in the calculation of the wave function for each state, and non-orthogonality was taken in account in transition probabilities calculations.

In order to obtain a correct relationship between many-body methods and quantum electrodynamics (QED) [17, 18, 19, 20], one should start from the no-pair Hamiltonian

$$\mathcal{H}^{\text{no pair}} = \sum_{i=1}^N \mathcal{H}_D(r_i) + \sum_{i<j} \mathcal{V}(|\mathbf{r}_i - \mathbf{r}_j|), \quad (1)$$

where  $\mathcal{H}_D$  is the one electron Dirac operator and  $\mathcal{V}$  is an operator representing the electron-electron interaction of order one in  $\alpha$ , properly set up between projection operators  $A_{ij}^{++} = A_i^+ A_j^+$  to avoid coupling positive and negative energy states

$$\mathcal{V}_{ij} = A_{ij}^{++} V_{ij} A_{ij}^{++}. \quad (2)$$

The expression of  $V_{ij}$  in the Coulomb gauge and in atomic units is

$$V_{ij} = \frac{1}{r_{ij}} \quad (3a)$$

$$- \frac{\boldsymbol{\alpha}_i \cdot \boldsymbol{\alpha}_j}{r_{ij}} \quad (3b)$$

$$- \frac{\boldsymbol{\alpha}_i \cdot \boldsymbol{\alpha}_j}{r_{ij}} \left[ \cos\left(\frac{\omega_{ij} r_{ij}}{c}\right) - 1 \right] + c^2 (\boldsymbol{\alpha}_i \cdot \nabla_i) (\boldsymbol{\alpha}_j \cdot \nabla_j) \frac{\cos\left(\frac{\omega_{ij} r_{ij}}{c}\right) - 1}{\omega_{ij}^2 r_{ij}}, \quad (3c)$$

where  $r_{ij} = |\mathbf{r}_i - \mathbf{r}_j|$  is the inter-electronic distance,  $\omega_{ij}$  is the energy of the photon exchanged between the two electrons,  $\boldsymbol{\alpha}_i$  are the Dirac matrices and  $c = 1/\alpha$  is the speed of light,  $\alpha$

being the fine structure constant. We use the Coulomb gauge as it has been demonstrated that it provides energies free from spurious contributions at the ladder approximation level and must be used in many-body atomic structure calculations [21, 22].

The term (3a) represents the Coulomb interaction, the term (3b) is the Gaunt (magnetic) interaction, and the last two terms (3c) stand for the retardation operator. In this expression the  $\nabla$  operators act only on  $r_{ij}$  and not on the following wave functions.

By a series expansion of the operators in expressions (3b) and (3c) in powers of  $\omega_{ij}r_{ij}/c \ll 1$  one obtains the Breit interaction, which includes the leading retardation contribution of order  $1/c^2$ . The Breit interaction is, then, the sum of the Gaunt interaction (3b) and the Breit retardation

$$B_{ij}^R = \frac{\boldsymbol{\alpha}_i \cdot \boldsymbol{\alpha}_j}{2r_{ij}} - \frac{(\boldsymbol{\alpha}_i \cdot \mathbf{r}_{ij})(\boldsymbol{\alpha}_j \cdot \mathbf{r}_{ij})}{2r_{ij}^3}. \quad (4)$$

In the many-body part of the calculation the electron-electron interaction is described by the sum of the Coulomb and the Breit interactions. Higher orders in  $1/c$ , deriving from the difference between Eqs. (3c) and (4) are treated here only as a first order perturbation.

All calculations are done for finite nuclei using uniformly charged spheres.

Finally, from a full QED treatment, one also obtains the radiative corrections (important for the innermost shells) to the electron-nucleus interaction (self-energy and vacuum polarization). The one-electron self-energy is evaluated using the one-electron values of Mohr and coworkers [23, 24, 25]. The self-energy screening is treated with the Welton method developed in Refs. [26, 27, 28, 29]. This method yields results in close agreement (better than 5%) with *ab initio* methods based on QED [30, 31, 32], without the huge amount of effort involved. The vacuum polarization is evaluated as described in Ref. [33]. The Uehling contribution is evaluated to all orders by being included in the self-consistent field (SCF). The Wichmann and Kroll and Källén and Sabry contributions are included perturbatively. All three contributions are evaluated using the numerical procedure from Refs. [34, 35].

Breit and QED contributions to the energy of some levels are shown in Table I for Mg, Ca and Zn.

### III. RESULTS

We calculated the energies of the  $K\alpha^h$  hypersatellite transitions and the  $K\alpha\alpha$  two-electron one-photon transitions for atoms with  $12 \leq Z \leq 30$ .

Depending on the configurations of the initial and final states, for the different values of  $Z$ , the number of transitions that must be dealt with may range from only two, when the initial state has only closed shells, to several hundred, when unfilled shells exist.

For Mg, Ar, Ca and Zn the  $1s^{-2}$  ground configuration corresponds to only one level, the  $^1S_0$  level, and each of the  $K\alpha\alpha$  or  $K\alpha^h$  lines is identified by a precise level transition,

$$\begin{aligned} K\alpha_2\alpha_3: & \quad 1s^{-2} \ ^1S_0 \rightarrow 2s^{-1}2p^{-1} \ ^1P_1 \\ K\alpha_1\alpha_3: & \quad 1s^{-2} \ ^1S_0 \rightarrow 2s^{-1}2p^{-1} \ ^3P_1 \\ K\alpha_2^h: & \quad 1s^{-2} \ ^1S_0 \rightarrow 1s^{-1}2p^{-1} \ ^1P_1 \\ K\alpha_1^h: & \quad 1s^{-2} \ ^1S_0 \rightarrow 1s^{-1}2p^{-1} \ ^3P_1 \end{aligned}$$

To be able to compare our theoretical transition energy values with experiment and non-relativistic calculations by other authors, we must define the statistical average energy of a line. The energy of all individual  $i \rightarrow f$  transitions in the  $X$  line, from an initial level  $i$ ,  $E_{if}$ , weighted by the corresponding transition probability,  $W_{if}$ , yields the average energy of the  $X$  line coming from level  $i$ ,  $E_X(i)$ :

$$E_X(i) = \frac{\sum_{f(X)} E_{if} W_{if}}{\sum_{f(X)} W_{if}} \quad (5)$$

In Eq. (5),  $f(X)$  runs over all possible final levels in the radiative de-excitation leading to the  $X$  line, from a specific initial level  $i$ . Assuming that all states of a  $\gamma$  configuration are equally populated, the resulting  $E_X(i)$  energies were then weighted by the statistical weight of level  $i$ ,  $g(i)$ , leading to the statistical average energy  $E_X^{\text{SA}}$  for the  $X$  line:

$$E_X^{\text{SA}} = \frac{1}{g(\gamma)} \sum_i g(i) E_X(i). \quad (6)$$

Here,  $g(\gamma)$  is the statistical weight of the  $\gamma$  configuration. We estimate the uncertainty of transition energy values has being of the order of 1 eV.

In Table II, we tabulate the results obtained in this work for the two-electron one-photon radiative transition energies and probabilities from a double K-hole state in aluminium. In this table, the transitions in the  $K\alpha\alpha$  lines were ordered by energy: two groups of transitions well separated in energy are clearly identified, which we interpret as being the  $K\alpha_2\alpha_3$  and  $K\alpha_1\alpha_3$  lines, respectively. Further details can be found in [36]. Afterwards, the transitions were grouped, within each of these two groups of transitions, by their initial level, either

${}^2P_{1/2}$  or  ${}^2P_{3/2}$ . Transition probabilities for all  $K\alpha\alpha$  two-electron one-photon transitions in aluminium are shown in Fig. 2.

As can be seen in Table II, for aluminium the values of the average energy  $E_X$  for transitions starting from different initial levels are very similar. This is also evident in Table III, where the average energy values of the x-ray lines for different initial levels of titanium are presented. It is worth mentioning that 401 transition energies were computed to obtain the results corresponding to the  $K\alpha\alpha$  lines of the latter case.

To avoid time-consuming calculations, some authors have calculated just the  $2s^22p^6 \rightarrow 1s^22s2p^5$  transition energy for all values of  $Z$ , thus neglecting the interaction with the outer electrons. To check the magnitude of the error arising from this simplification, we calculated the transition energies for the atoms with  $Z = 12, 13, 18, 20, 21, 22, 28, 30$ , first taking in account all electrons and, in a separate calculation, including in the initial configuration only electrons in the L-shell.

For example, in the case of aluminium  $K\alpha\alpha$  lines, we calculated the transition energy for both the  $2s^22p^63s^23p \rightarrow 1s^22s2p^53s^23p$  and the  $2s^22p^6 \rightarrow 1s^22s2p^5$  transitions. In the particular case of  $K\alpha_2\alpha_3$ , we found a 6.8 eV energy difference between the two energy values, out of the 3056.54 eV transition energy (a difference of 0.2 %). Table IV gives the energy values of the  $K\alpha_2\alpha_3$  line for the 8 elements considered, obtained through the two approaches described. The energy differences,  $\Delta E_{th}$ , thus obtained were then fitted to a straight line as a function of  $Z$  (Fig. 3). We found that the fit is quite good, presenting a correlation coefficient of 0.998. Using the results of this fitting process, and calculations where only the  $2s^22p^6$  electrons were included in the initial states, we obtained  $K\alpha_2\alpha_3$  transition energies for the atoms with the remaining  $Z$  values.

Similar behaviour is also observed from the other lines obtained in the decay of a double K-hole state ( $K\alpha_1\alpha_3$ ,  $K\alpha_2^h$ ,  $K\alpha_1^h$ ). Thus, using the same method, we were able to obtain the transition energy values for other atoms, with values of  $Z$  between 12 and 30, for which complete calculations would involve time-consuming work. For example, for iron ( $Z = 26$ ) it would be necessary to calculate around five thousand transition energy values to obtain the energy of the  $K\alpha_2^h$  and  $K\alpha_1^h$  hypersatellite or  $K\alpha_2\alpha_3$  and  $K\alpha_1\alpha_3$  lines.

The results, for all elements with  $12 \leq Z \leq 30$ , are presented in Table V and Table VI, where they are compared with other theoretical calculations and experimental values. A comparison between the results of this work for  $K\alpha_2^h$  line energies and other available results

is presented in Fig. 4.

#### IV. DISCUSSION AND CONCLUSIONS

In this work, we computed the energy of  $K\alpha_2^h$ ,  $K\alpha_1^h$ ,  $K\alpha_2\alpha_3$  and  $K\alpha_1\alpha_3$  lines in the framework of the Dirac-Fock approximation for elements with atomic number  $12 \leq Z \leq 30$ . For selected elements we performed two different calculations: first we took  $1s^{-2}$  as the initial configuration, then we repeated the calculation, considering the  $2s^22p^6$  configuration as the initial one. We fitted the differences between the values obtained in the two calculations, as a function of  $Z$ , to a straight line. We used this result to make a correction to the energies of the remaining elements calculated using the  $2s^22p^6$  configuration as the initial one.

These results can be compared with experimental work in which K-holes were obtained using electron bombardment, photo ionization or radioactive decay. Other methods of producing K shell holes, like ion bombardment, will inevitably produce extra holes in the atom, leading to shifts in the measured value of the transition energy, unless the resolution obtained with the detection process is high enough to allow for separation of the peaks resulting from multiple vacancies.

The values obtained in this work for the  $K\alpha_2^h$  and  $K\alpha_1^h$  line energies are in excellent agreement with the experimental results (see Fig. 4 for  $K\alpha_2^h$  energies). We particularly emphasize the agreement with the measured  $K\alpha_2^h$  energy value of Mikkola et al. [37], for  $Z = 12$ , Keski-Rahkonen et al. [38] for  $Z = 13$ , , and Diamant et al. [39], for  $Z = 29$ , due to the reported high experimental precision. These authors resolved the x-ray lines using crystal spectrometers.

In Table V we present a comparison between our calculated values and the available experimental and theoretical data, in particular those obtained by Chen et al. [14] in the framework of the Dirac-Hartree-Slater (DHS) method for  $Z = 18, 20, 25$  and  $30$ . The differences between the present calculations and the DHS calculations are probably due mainly to the differences in wave functions (ours were obtained with the optimized level (OL) method and the DHS ones with the configuration-average level method). Additionally, we used an electron-electron operator that avoids coupling between positive and negative states, and we included higher orders in  $1/c$  of the Breit interaction.

Our results are closer to experiment than other theoretical results for the  $K\alpha_2\alpha_3$  line;

no previous calculation has been reported, to our knowledge, for the  $K\alpha_1\alpha_3$  line. A more detailed comparison with the available experimental results reveals that, for  $24 \leq Z \leq 29$ , our values lie systematically higher (between 0.2% and 0.4%) than the experimental values, outside the reported experimental uncertainty in all cases [9, 10]. Regarding the value of Auerhammer et al. [7] for the Al ( $Z = 13$ )  $K\alpha_2\alpha_3$  line, some comments are in order. These authors report the  $K^{-2} \rightarrow L^{-2}$  two-electron one-photon lines as well as the  $K^{-2}L^{-n} \rightarrow L^{-(2+n)}$  satellite lines, with  $n = 1, \dots, 4$ . They used the calculated values of Tannis et al. [40] to propose the identification of most of their measured transition lines. The line with energy difference  $\Delta E = E(K\alpha\alpha) - 2E(K\alpha_1) = 103.4$  eV was labelled by them as the  $K\alpha_2\alpha_3$  line. We suggest that this label should be attributed instead to their unidentified line with energy  $\Delta E = 84.8$  eV, in much closer agreement with our calculated value  $\Delta E = 82.2$  eV.

### Acknowledgments

This research was supported in part by FCT project POCTI/FAT/50356/2002 financed by the European Community Fund FEDER.

- 
- [1] J. P. Briand, L. d. Billy, P. Charles, S. Essabaa, P. Briand, R. Geller, J. P. Desclaux, S. Bliman, and C. Ristori, *Phys. Rev. Lett.* **65**, 159 (1990).
  - [2] K. Moribayashi, A. Sasaki, and T. Tajima, *Phys. Rev. A* **58**, 2007 (1998).
  - [3] W. Heisenberg, *Z. Phys.* **32**, 841 (1925).
  - [4] E. U. Condon, *Phys. Rev.* **36**, 1121 (1930).
  - [5] W. Wölffi, C. Stoller, G. Bonani, M. Suter, and M. Stöckli, *Phys. Rev. Lett.* **35**, 656 (1975).
  - [6] C. Stoller, W. Wölffi, G. Bonani, M. Stöckli, and M. Suter, *Phys. Rev. A* **15**, 990 (1977).
  - [7] J. Auerhammer, H. Genz, A. Kumar, and A. Richter, *Phys. Rev. A* **38**, 688 (1988).
  - [8] S. I. Salem, A. Kumar, B. L. Scott, and R. D. Ayers, *Phys. Rev. Lett.* **49**, 1240 (1982).
  - [9] S. I. Salem, A. Kumar, and B. L. Scott, *Phys. Rev. A* **29**, 2634 (1984).
  - [10] Y. Isozumi, *Phys. Rev. A* **22**, 1948 (1980).
  - [11] A. R. Knudson, K. W. Hill, P. G. Burkhalter, and D. J. Nagel, *Phys. Lett.* **37**, 679 (1976).



- [12] M. Gavrilă and J. E. Hansen, *J. Phys. B* **11**, 1353 (1978).
- [13] T. K. Mukherjee and P. K. Mukherjee, *Z. Phys. D* **42**, 29 (1997).
- [14] M. H. Chen, B. Crasemann, and H. Mark, *Phys. Rev. A* **25**, 391 (1982).
- [15] J. P. Desclaux, *Comp. Phys. Commun.* **9**, 31 (1975).
- [16] P. Indelicato, *Phys. Rev. Lett.* **77**, 3323 (1996).
- [17] P. Indelicato, *Phys. Rev. A* **51**, 1132 (1995).
- [18] G. E. Brown and D. E. Ravenhall, *Proc. R. Soc. London, Ser. A* **208**, 552 (1951).
- [19] J. Sucher, *Phys. Rev. A* **22**, 348 (1980).
- [20] M. H. Mittleman, *Phys. Rev. A* **24**, 1167 (1981).
- [21] O. Gorceix and P. Indelicato, *Phys. Rev. A* **37**, 1087 (1988).
- [22] E. Lindroth and A.-M. Mårtensson-Pendrill, *Phys. Rev. A* **39**, 3794 (1989).
- [23] P. J. Mohr, *Phys. Rev. A* **26**, 2338 (1982).
- [24] P. J. Mohr and Y.-K. Kim, *Phys. Rev. A* **45**, 2727 (1992).
- [25] P. J. Mohr, *Phys. Rev. A* **46**, 4421 (1992).
- [26] P. Indelicato, O. Gorceix, and J. P. Desclaux, *J. Phys. B* **20**, 651 (1987).
- [27] P. Indelicato and J. P. Desclaux, *Phys. Rev. A* **42**, 5139 (1990).
- [28] P. Indelicato and E. Lindroth, *Phys. Rev. A* **46**, 2426 (1992).
- [29] P. Indelicato, S. Boucard, and E. Lindroth, *Eur. Phys. J. D* **3**, 29 (1998).
- [30] P. Indelicato and P. J. Mohr, *Theor. Chim. Acta* **80**, 207 (1991).
- [31] S. A. Blundell, *Phys. Rev. A* **46**, 3762 (1992).
- [32] S. A. Blundell, *Phys. Scr.* **T46**, 144 (1993).
- [33] S. Boucard and P. Indelicato, *Eur. Phys. J. D* **8**, 59 (2000).
- [34] S. Klarsfeld, *Phys. Lett.* **30A**, 382 (1969).
- [35] L. W. Fullerton and J. G. A. Rinkler, *Phys. Rev. A* **13**, 1283 (1976).
- [36] J. P. Santos, M. C. Martins, A. M. Costa, P. Indelicato, and F. Parente, *Nucl. Instr. and Meth. in Phys. Res. B* **205**, 107 (2003).
- [37] E. Mikkola, O. Keski-Rahkonen, and R. Kuoppala, *Phys. Scr.* **19**, 29 (1979).
- [38] O. Keski-Rahkonen, E. Mikkola, K. Reinikainen, and M. Lehkonen, *J. Phys. C* **18**, 2961 (1985).
- [39] R. Diamant, S. Huotari, K. Hämäläinen, C. C. Kao, and M. Deutsch, *Phys. Rev. A* **62**, 052519 (2000).

- [40] J. A. Tanis, J. M. Feagin, W. W. Jacobs, and S. M. Shafroth, *Phys. Rev. Lett.* **38**, 868 (1977).
- [41] J. Ahopelto, E. Rantavuori, and O. Keski-Rahkonen, *Phys. Scr.* **20**, 71 (1979).
- [42] J. P. Briand, P. Chevallier, A. Johnson, J. P. Rozet, M. Tavernier, and A. Touati, *Phys. Lett. A* **49**, 51 (1974).
- [43] J. P. Briand, A. Touati, M. Frilley, P. Chevallier, A. Johnson, J. P. Rozet, M. Tavernier, S. Shafroth, and M. O. Krause, *J. Phys. B* **9**, 1055 (1976).
- [44] R. Diamant, S. Huotari, K. Hämäläinen, R. Sharon, C. C. Kao, and M. Deutsch, *Phys. Rev. Lett.* **91**, 193001 (2003).
- [45] H. J. Nagy and G. Schupp, *Phys. Rev. C* **27**, 2887 (1983).
- [46] K. N. Huang, M. Aoyagi, M. H. Chen, B. Crasemann, and H. Mark, *At. Data Nucl. Data Tables* **18**, 243 (1976).
- [47] R. D. Deslattes, E. G. Kessler, P. Indelicato, L. de Billy, E. Lindroth, and J. Anton, *Rev. Mod. Phys.* **75**, 35 (2003).
- [48] S. I. Salem, A. Kumar, and B. L. Scott, *Phys. Lett. A* **97**, 100 (1983).

TABLE I: QED and Breit contributions to the total energy,  $E$ , in eV, for Mg, Ca and Zn.

	Mg ( $Z=12$ )			Ca ( $Z=20$ )			Zn ( $Z=30$ )		
	$1s^{-2}$	$1s^{-1}2p^{-1}$	$2s^{-1}2p^{-1}$	$1s^{-2}$	$1s^{-1}2p^{-1}$	$2s^{-1}2p^{-1}$	$1s^{-2}$	$1s^{-1}2p^{-1}$	$2s^{-1}2p^{-1}$
	$^1S_0$	$^3P_1$	$^3P_1$	$^1S_0$	$^3P_1$	$^3P_1$	$^1S_0$	$^3P_1$	$^3P_1$
$E$	-2663.734	-4038.075	-5264.540	-10117.187	-14013.573	-17642.276	-29042.059	-37997.033	-46466.031
QED	0.057	0.327	0.549	0.420	1.989	3.311	1.878	8.015	13.235
Breit	0.139	0.249	0.820	1.010	1.822	4.748	4.886	8.158	18.454

TABLE II: Two-electron one-photon radiative transition energies ( $E_{if}$ ) and probabilities ( $W_{if}$ ) for the  $2s^2 2p^6 3s^2 3p \rightarrow 1s^2 2s 2p^5 3s^2 3p$  transition in aluminium.  $E_X$  is defined by Eq. (5) and  $E_X^{SA}$  is defined by Eq. (6). Superscripts  $\#^i$  are added to distinguish identical terms in the same configuration, where  $\#^1$  stands for the term with the lowest energy. The transition energy values are in eV.

Initial Level	Final Level	$E_{if}$	$W_{if}$ ( $s^{-1}$ )	$E_X$	$E_X^{SA}$			
$K\alpha_2\alpha_3$	$^2P_{1/2}$	$^2S_{1/2}\#^2$	3053.62	$2.79 \times 10^9$				
		$^2P_{3/2}\#^2$	3056.45	$9.53 \times 10^9$				
		$^2P_{1/2}\#^2$	3056.47	$2.36 \times 10^{10}$				
	$^2P_{3/2}$	$^2D_{3/2}\#^2$	3057.02	$5.78 \times 10^{10}$	3056.72			
		$^2S_{1/2}\#^2$	3053.72	$1.17 \times 10^{10}$				
		$^2P_{3/2}\#^2$	3056.52	$2.87 \times 10^{10}$				
		$^2P_{1/2}\#^2$	3056.54	$4.97 \times 10^9$				
		$^2D_{5/2}\#^2$	3056.97	$5.02 \times 10^{10}$				
		$^2D_{3/2}\#^2$	3057.09	$4.69 \times 10^9$	3056.45	3056.54		
		$K\alpha_1\alpha_3$	$^2P_{1/2}$	$^2S_{1/2}\#^1$	3071.68	$5.06 \times 10^7$		
				$^2P_{1/2}\#^1$	3073.19	$4.54 \times 10^5$		
				$^2P_{3/2}\#^1$	3073.25	$1.11 \times 10^5$		
				$^2D_{3/2}\#^1$	3073.47	$7.41 \times 10^5$		
				$^4P_{1/2}$	3073.61	$2.87 \times 10^5$		
$^4P_{3/2}$	3073.65			$8.59 \times 10^4$				
$^4D_{1/2}$	3074.21			$4.77 \times 10^5$				
$^4D_{3/2}$	3074.29			$1.64 \times 10^6$				
$^2P_{3/2}$	$^4S_{3/2}$		3075.50	$1.45 \times 10^5$	3071.85			
	$^2S_{1/2}\#^1$		3071.75	$3.71 \times 10^7$				
	$^2P_{1/2}\#^1$		3073.26	$5.44 \times 10^6$				
	$^2P_{3/2}\#^1$		3073.32	$3.78 \times 10^6$				
	$^2D_{3/2}\#^1$		3073.54	$5.61 \times 10^4$				
	$^4P_{1/2}$		3073.68	$6.84 \times 10^3$				
	$^2D_{5/2}\#^1$	3073.69	$7.90 \times 10^5$					
	$^4P_{3/2}$	3073.72	$1.17 \times 10^6$					
	$^4P_{5/2}$	3073.76	$6.48 \times 10^5$					
	$^4D_{1/2}$	3074.28	$1.63 \times 10^5$					
	$^4D_{3/2}$	3074.36	$1.12 \times 10^5$					
	$^4D_{5/2}$	3074.48	$9.99 \times 10^5$					
	$^4S_{1/2}$	3075.57	$3.68 \times 10^5$	3072.23	3072.10			

TABLE III: Titanium two-electron one-photon radiative transition average energies in eV of the  $X$  line coming from the initial level.  $E_X^{SA}$  is defined by Eq. (6).

	Initial Level	$E_X$	$E_X^{SA}$
K $\alpha_2\alpha_3$	$^3P_0$	9144.96	
	$^1S_0$	9144.93	
	$^3P_1$	9144.99	
	$^3F_2$	9144.97	
	$^1D_2$	9144.97	
	$^3P_2$	9145.05	
	$^3F_3$	9145.04	
	$^3F_4$	9145.12	
	$^1G_4$	9145.05	9145.04
K $\alpha_1\alpha_3$	$^3P_0$	9174.22	
	$^1S_0$	9175.64	
	$^3P_1$	9174.42	
	$^3F_2$	9173.64	
	$^1D_2$	9173.98	
	$^3P_2$	9175.19	
	$^3F_3$	9174.20	
	$^3F_4$	9175.37	
	$^1G_4$	9175.29	9174.72

TABLE IV: Transition energies in eV for K $\alpha_2\alpha_3$  calculated using all electrons ( $E_X^{SA}$ ) and using only the  $2s^2 2p^6$  electrons ( $E^*$ ), respectively.  $\Delta E_{th}$  indicates the difference between these energy values:  $\Delta E_{th} = E^* - E_X^{SA}$ .

$Z$	Initial Configuration	$E_X^{SA}$	$E^*$	$\Delta E_{th}$
12	$2s^2 2p^6 3s^2$	2585.45	2589.01	3.56
13	$2s^2 2p^6 3s^2 3p$	3056.54	3063.37	6.83
18	$2s^2 2p^6 3s^2 3p^6$	6022.29	6056.94	34.65
20	$2s^2 2p^6 3s^2 3p^6 4s^2$	7497.79	7546.10	48.31
21	$2s^2 2p^6 3s^2 3p^6 3d 4s^2$	8300.74	8353.62	52.88
22	$2s^2 2p^6 3s^2 3p^6 3d^2 4s^2$	9145.04	9203.25	58.21
28	$2s^2 2p^6 3s^2 3p^6 3d^8 4s^2$	15098.34	15193.17	94.83
30	$2s^2 2p^6 3s^2 3p^6 3d^{10} 4s^2$	17423.97	17533.31	109.34

TABLE V:  $K\alpha_2^h$  and  $K\alpha_1^h$  theoretical and experimental transition energies in eV. The superscripts stand for: a-Ref. [37], b-Ref. [38], c-Ref. [41], d-Ref. [9], e-Ref. [42, 43], f-Ref. [39, 44] and g-Ref. [45]. Since the  $K\alpha_{1,2}^h$  theoretical values obtained by Chen et al. [14] were presented in the form of energy shifts from the corresponding diagram lines, we used the  $K\alpha_{1,2}$  energy values calculated by the same authors [46] in order to obtain the  $K\alpha_1^h$  and the  $K\alpha_2^h$  transition energies. An asterisk indicates that the authors presented experimental results as energy shifts from the corresponding diagram line. In these cases we took the diagram line energy values from [47].

$Z$	$K\alpha_2^h$					$K\alpha_1^h$		
	Theory			Experiment	Theory		Experiment	
	MCDF	Fitted	Ref. [13]		Ref. [12]	Ref. [14]		MCDF
12	1368.53		1381			1367.8±0.2 <sup>a</sup>	1374.34	
13	1611.75		1627	1608		1610.8±0.2 <sup>b*</sup>	1616.69	
14		1874	1893				1880	
15		2157	2179				2164	
16		2461	2487				2469	
17		2785	2816	2777			2794	
18	3131.50	3164			3130.9		3141.62	3141.7
19		3498					3508	
20	3884.80			3864	3884.4		3896.39	3896.8
21	4294.16						4306.27	
22	4723.86					4727±2 <sup>c</sup>	4736.76	4741±3 <sup>c</sup>
23		5174					5188	
24		5647				5650±2 <sup>c</sup> 5645±2 <sup>d</sup>	5662	5666±3 <sup>c</sup>
25		6140			6140.1	6160±20 <sup>e</sup>	6156	6158.0
26		6655		6597		6659±2 <sup>c</sup> 6655±2 <sup>d</sup> 6658±2 <sup>e*</sup> 6658.31±0.10 <sup>f</sup>	6673	6679±3 <sup>c</sup> 6675±2 <sup>d</sup> 6677.36±0.18 <sup>f</sup>
27		7191				7192±3 <sup>d</sup>	7211	7207±3 <sup>d</sup>
28	7749.04			7670		7751±2 <sup>c</sup> 7752±3 <sup>e*</sup>	7770.90	7775±3 <sup>c</sup>
29		8328				8331±3 <sup>d</sup> 8331±3 <sup>e*</sup> 8329.5±0.3 <sup>f*</sup> 8362±17 <sup>g</sup>	8352	8352±3 <sup>d</sup> 8353.1±0.7 <sup>f</sup>
30	8928.53				8928.7		8954.97	8955.4

TABLE VI:  $K\alpha_2\alpha_3$  and  $K\alpha_1\alpha_3$  theoretical and experimental transition energies in eV. The superscripts stand for: a-Ref. [7], b-Ref. [9, 48] and c-Ref. [10].

Z	$K\alpha_2\alpha_3$				$K\alpha_1\alpha_3$	
	Theory			Experiment	Theory	
	MCDF	Fitted	Ref. [13]		Ref. [12]	MCDF
12	2585.45		2653			2600.81
13	3056.54		3188	3051	3076.8 <sup>a</sup>	3072.10
14		3566	3673			3584
15		4118	4240			4137
16		4710	4848			4731
17		5345	5489	5333		5367
18	6022.29		6178			6046.71
19		6378				6764
20	7497.79			7464		7525.09
21	8300.74					8328.97
22	9145.04					9174.72
23		10029				10060
24		10958			10935±8 <sup>b</sup>	10990 10960±8 <sup>b</sup>
25		11929			11907±20 <sup>c</sup>	11962
26		12942		12483	12907±9 <sup>b</sup>	12978 12953±9 <sup>b</sup>
27		13999			13945±10 <sup>b</sup>	14036 14005±10 <sup>b</sup>
28	15098.34			14960	15060±10 <sup>b</sup>	15136.33 15108±10 <sup>b</sup>
29		16240			16193±10 <sup>b</sup>	16281 16236±10 <sup>b</sup>
30	17423.97					17466.82

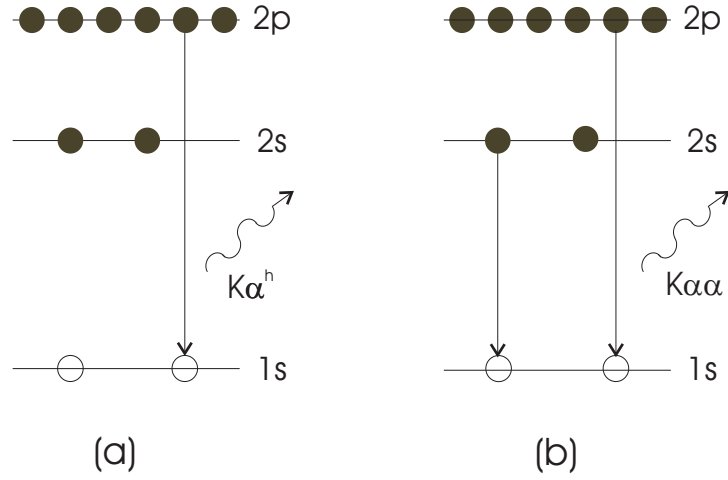


FIG. 1: (a) One-electron one-photon transition that produces the  $K\alpha^h$  hypersatellite lines; (b) two-electron one-photon transition that produces the  $K\alpha\alpha$  lines.

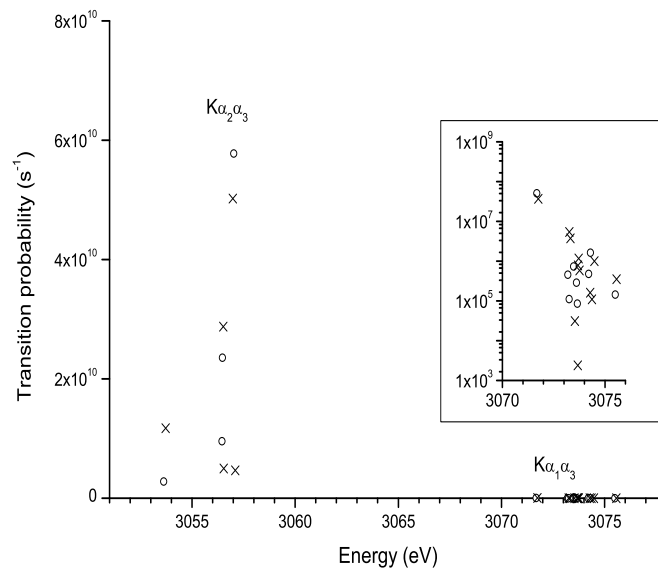


FIG. 2: Transition probabilities for all  $K\alpha\alpha$  two-electron one-photon transitions in aluminium. The transitions for the initial levels  $^2P_{1/2}$  and  $^2P_{3/2}$  are represented, respectively, by ○ and ×.



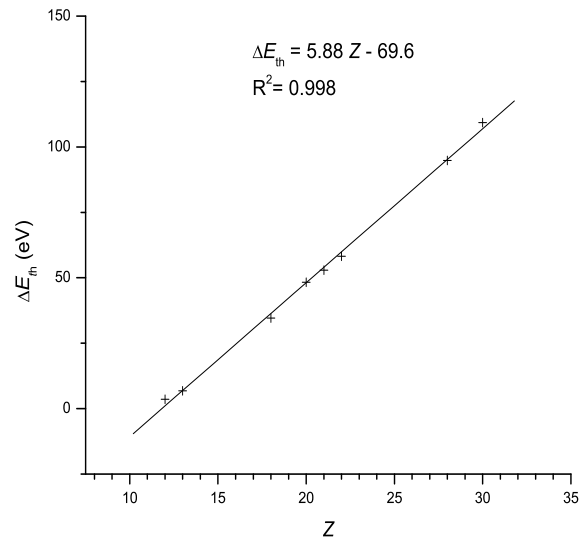


FIG. 3: The differences  $\Delta E_{\text{th}}$ , as a function of atomic number  $Z$ , between the transition energies calculated for the  $K\alpha_2\alpha_3$  line, using only the  $2s^2 2p^6$  configuration and using the  $1s^{-2}$  configuration (+). The straight line represents the linear regression to these energy differences.

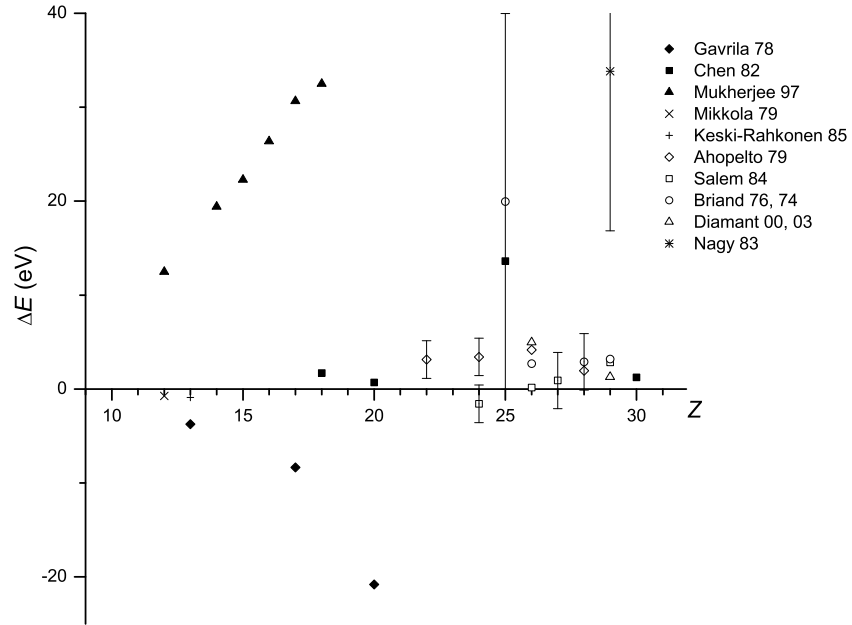


FIG. 4: Comparison between available calculated and measured values of  $K\alpha_2^h$  energy and those of the present work, for  $12 \leq Z \leq 30$ .  $\Delta E$  stands for the difference between other energy values and the values obtained in this work.